Clays and Clay Minerals, Vol. 23, pp. 355–360. Pergamon Press 1975. Printed in Great Britain

ELECTRON-MICROSCOPIC AND MÖSSBAUER SPECTROSCOPIC STUDIES OF IRON-STAINED KAOLINITE MINERALS

D. A. JEFFERSON, M. J. TRICKER and A. P. WINTERBOTTOM

Edward Davies Chemical Laboratories, Aberystwyth, SY23 1NE, U.K.

(*Received* 26 *December* 1974; *Revised form* 24 *June* 1975)

Abstract—An electron-microscopic and Mössbauer spectroscopic study of a range of kaolinites has revealed three distinct types of iron contamination within these minerals: a) Ferric ion may substitute for aluminium and be evenly distributed throughout the lattice. b) Ferric ion may be present as a crystalline coating of goethite, as indicated by lattice-imaging studies, or c) as an amorphous coating. The distribution of the iron in the groups *b* and *c* is non-uniform and is highest at the flake surfaces. Ferrous ion, when detected, is thought to be evenly distributed throughout the lattice. The size of the contaminating goethite crystallites and the observed Mössbauer spectra of these samples suggest that such particles are super-paramagnetic. All kaolinites can be cleaned by acid treatment except those having iron substituting for Al^{3+}.

INTRODUCTION

The minerals of the kaolinite group are of considerable industrial importance and many processes require that the clay mineral is relatively pure and stain-free. The kaolinites have been widely studied (see for example the survey of Bates, 1971) by electron-optical methods, in both the scanning and transmission modes, chiefly in order to obtain morphological information. However most studies have concentrated on relatively pure kaolinites and little is known about the detailed nature and origin of the iron staining often associated with kaolinite deposits. As part of a general study of the ultra-microstructure and chemical properties of the kaolinite/illite/montmorillonite minerals, stained kaolinites from a variety of locations listed in Table 1 have been examined in considerable electron-microscopic detail. As it is generally thought that the stains may contain iron oxides or oxy-hydroxides ^{57}Fe Mössbauer spectroscopy has been used to further characterise the staining. Results of stain-removal experiments relevant to possible industrial methods are also reported.

EXPERIMENTAL

Each of the kaolinite samples was purified by sedimentation, the <2 micron fraction being selected for study. Portions of each sample were acid-extracted to investigate the rate of contaminant removal, the severity of the contamination requiring strong (30% wt) hydrochloric acid, although a weaker acid would have involved less risk of chemical attack on the kaolinite itself. All samples were left in contact with the acid for twenty-one days, apparent percentages of extractable iron being determined gravimetrically by conversion to Fe_2O_3.

Portions of untreated and acid-extracted samples were subsequently examined on a Phillips X-ray diffractometer and Guinier camera, using pressed, rather than sedimented specimens. For transmission electron microscopy, specimens were lightly ground in acetone suspension and deposited onto holey carbon film/copper grid mounts, and examined at intermediate and high magnifications in a Phillips EM–300 electron microscope, and in the scanning transmission mode in a J.E.O.L. JEM–100B analytical electron microscope. Lattice fringes, where recorded, were measured on an optical diffractometer by comparison with those from carbon black at the same magnification.

^{57}Fe Mössbauer spectra were also recorded for all samples prior to and following acid extraction, at 290°K. For reasons outlined later the sample CCBH7 was further studied at intermediate temperatures. A Harwell spectrometer of the constant acceleration type and a 10 mC source of ^{57}Co Rh was used, the spectrometer being periodically calibrated with an iron foil standard.

RESULTS

Acid extraction and X-ray diffractometry

Results from the acid-extraction tests are summarised in Table 1, the rate and extent of extraction varying from complete and rapid in the case of GP2 to incomplete and very slow in the case of the two South Carolina samples. X-ray diffractometer examination showed little difference between any of the samples, the only observable impurity being an illite-like material, occurring in all but the two South Carolina kaolinites. The latter were also the only samples to show clearly the *b*-axis disorder (Brindley, 1961) characteristic of certain kaolinites, shown by broad

Table 1. Extraction data for kaolinite samples. The two unstained samples (GP1 and TB146) used for comparison in the electron-microscopic study are omitted

Samples and origin	Extraction	Wt. % Fe extracted
TB153 Cornwall	slow	not determined
TB169 Cornwall	„	0·462
CCBH7 Spain	„	2·459
LBH22 Portugal	„	0·956
LBH23 Portugal	„	1·360
TPC1 Cornwall	„	0·526
GP2 Cornwall	rapid	0·725
BSC1 S. Carolina	incomplete	0·923
DRP1 S. Carolina	„	0·973

(hkl) diffraction bands. No peaks due to oxides or oxyhydroxides of iron were observed in the traces, or in a subsequent examination using a Guinier camera. In addition, no significant differences were noted in traces taken from untreated and acid-extracted portions of any one sample, except for a slight variation in the background level from the more iron-rich specimens (CCBH7 and TB153).

Electron microscopy

Transmission electron microscopy at intermediate magnifications revealed a considerable variation of flake shapes and sizes in all samples, with all but a small proportion of flakes examined having characteristically sharp and well-defined edges. Examination of flakes with irregular outlines in the analytical electron microscope suggested that they contained potassium, and were probably the illite-like impurity observed by X-ray powder diffraction. When micrographs of samples before and after extraction were compared, no differences were noted in the samples DRP1, BSC1, TPC1 and LBH23 which appeared to be identical to the unstained samples TB146 and GP1. One such micrograph is illustrated in Fig. 1(a).

Electron micrographs, taken at intermediate magnification, of the GP2 sample did show noticeable differences before and after acid extraction. In approximately 10% of all flakes studied before acid treatment, a peculiar form of mottled contrast on the flake basal surfaces was observed, as shown in Fig. 1(b). The observed high contrast suggests the presence of relatively heavy atoms, rather than an organic contaminant, and the close similarity between these micrographs and published ones of unaged ferric oxide gel (Mackenzie, Meldau and Gard, 1962) implied the presence of such a gel on the flake surfaces in this sample. A test examination of an originally unstained kaolinite with freshly precipitated ferric oxide gel on the flake surfaces was undertaken, giving remarkably similar micrographs to those of GP2. After acid extraction this form of contamination was found to be completely absent.

The remainder of the samples (TB153, TB169, LBH22 and CCBH7) showed fine, spindle-shaped surface particles on the untreated specimens. These were evidently associated with the staining, as they were not present in the acid extracted portions. These particles, which have no orientation relationship to the kaolinite lattice, were very similar to particles of natural goethite described by Mackenzie, Follet and Meldau (1971), although their outline was more irregular than that of the crystallites of synthetic goethite reported by the same authors. The presence of iron in the surface particles was confirmed by examination in the analytical electron microscope. In the two most heavily stained samples (TB153 and CCBH7) particles were observed on virtually every kaolinite flake (Fig. 1c), whereas less than 50% of all flakes were so contaminated in TB169 and LBH22. The latter often showed clumps of particles at flake edges (Fig. 1d: reminiscent of the tactoid structures observed in natural akaganéite by Mackay (1962). The small size of the contaminating particles prohibited the conventional recording of selected area diffraction patterns, although certain maxima additional to the normal kaolinite pattern were observed, and micro-beam diffraction (in the scanning transmission mode) caused the particles to decompose before a pattern could be recorded.

High resolution examination

As a result of the inability to record selected-area diffraction patterns from the contamination when observed, an attempt was made to characterise the contamination by recording and measuring lattice spacings in the high resolution mode of operation. Examination of the GP2 sample in this way revealed no definable crystal lattice (Fig. 2a), implying an amorphous type of contamination quite compatible with a gel structure. However, the samples with the fine particle type of contamination gave reasonable lattice images, indicative of a fair degree of crystallinity. The images were recorded at approximately 900Å under focus, giving a phase contrast transfer function (Erickson and Klug, 1971) which favoured resolution of spacings in the range 3·5 to 10·0Å for the particular spherical aberration coefficient ($C_s = 1{\cdot}6$ mm) of the instrument used.

The accuracy of the measured spacings was limited by the small size of the particles and hence the small number of fringes involved. Spacings of $4{\cdot}91 \pm 0{\cdot}11$Å (Fig. 2b) and $4{\cdot}34 \pm 0{\cdot}13$Å (Fig. 2c) were frequently recorded which reasonably correspond to goethite (020) and (110) lattice spacings, published values being 4·98Å and 4·18Å (Rooksby, 1961). In addition, spacings of $3{\cdot}6 \pm 0{\cdot}10$Å and $2{\cdot}7 \pm 0{\cdot}18$Å were recorded which either correspond to the (102) and (104) lattice spacings of hematite or the (120) and (130) spacings

https://doi.org/10.1346/CCMN.1975.0230505 Published online by Cambridge University Press

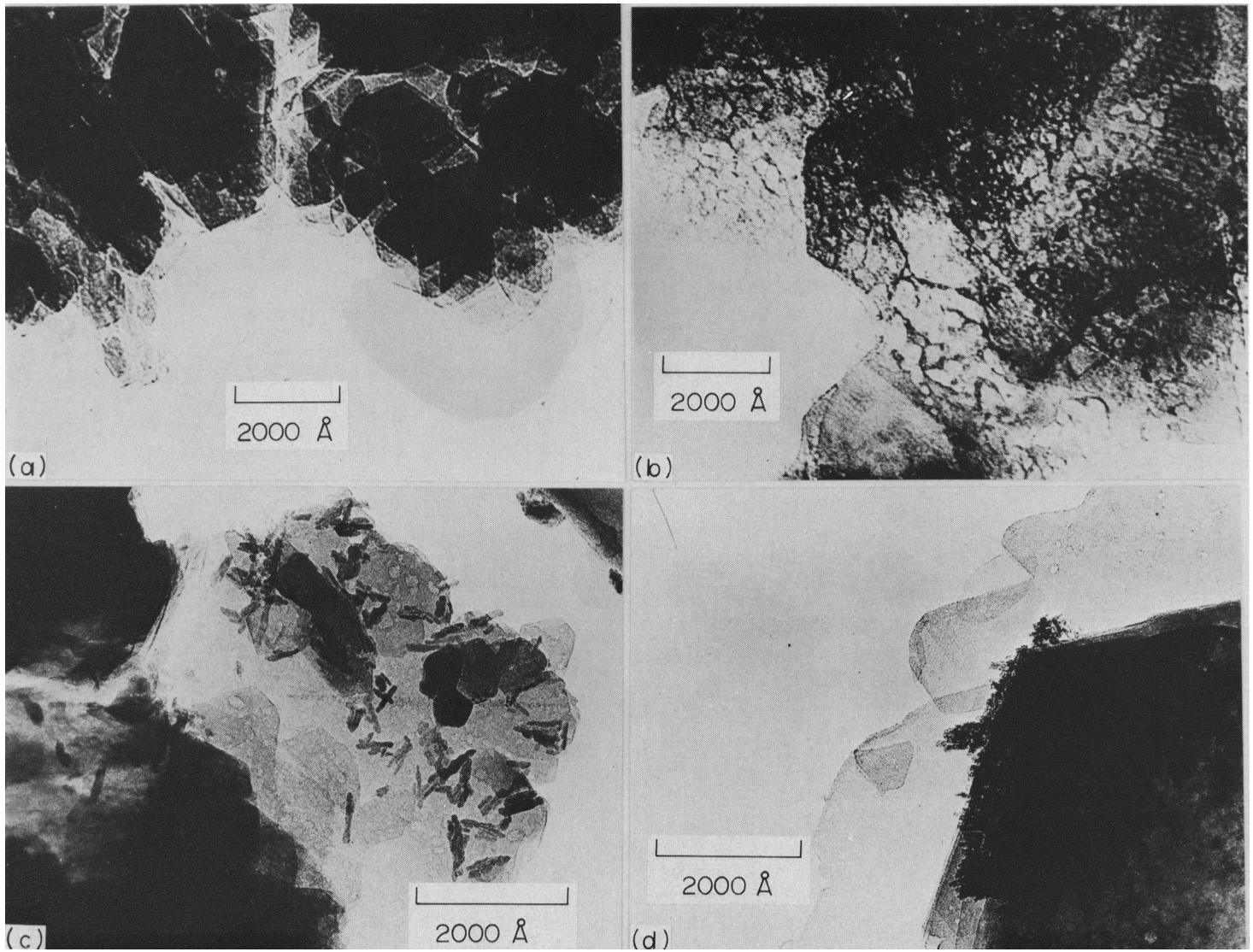

Fig. 1. (a) An unstained kaolinite (GP1) at intermediate magnification. (b) The stained GP2 sample at similar magnification, showing the mottled contrast effect. (c) the heavily stained CCBH7 sample, showing surface contaminating particles. (d) A clump of similar particles seen in the LBH22 sample.

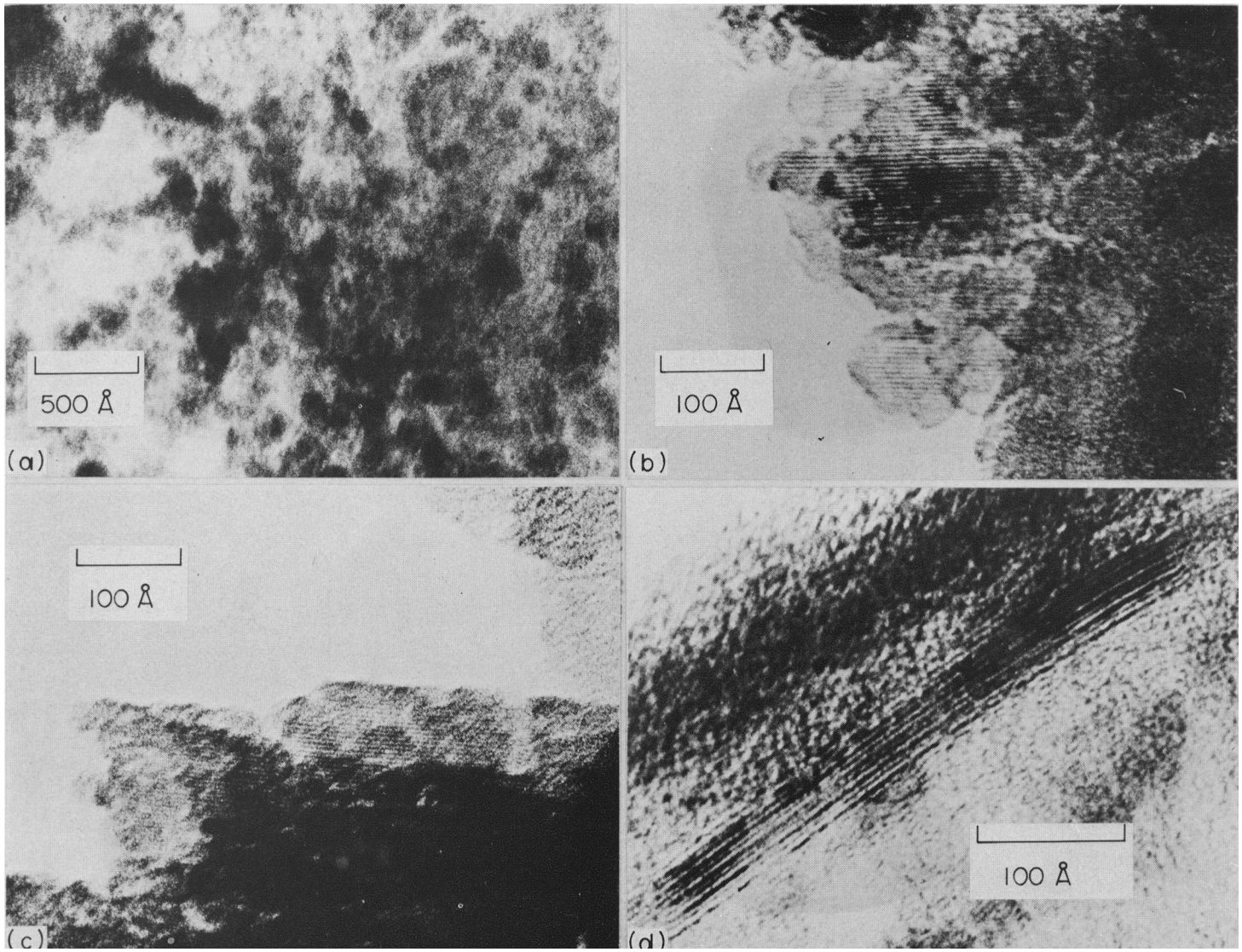

Fig 2. (a) High-resolution image of the amorphous coating of the GP2 sample. (b) Lattice image of a contaminating crystalline particle in sample CCBH7. The spacing corresponds to the (020) spacing of goethite. (c) Lattice image of a crystalline surface particle in sample TB153. The spacing corresponds to the (110) lattice spacing of goethite. (d) Lattice resolution at the edge of a (supposedly) kaolinite flake. The spacing in fact is approximately 10 Å.

of goethite. Previously published values of these spacings are 3·67Å and 2·69Å for hematite and 3·38Å and 2·69Å for goethite. As a result of this high resolution examination there is little doubt that the bulk of the contaminating material contributing to the staining was in fact goethite.

Lattice images were also obtained from the parent flakes in these samples. These show three systems of 4·6Å fringes mutually inclined at 60° and are very similar to those observed in phyrophyllite by Dowell (1961). Observation of simultaneous lattice images of this type, and lattice images in the contaminating particles, confirmed that the particles were disposed with no definite orientation to the kaolinite lattice. Lattice images (00*l*) of the main flakes also were obtained. These are similar to those observed in organo-montmorillonites by Suito, Arakawa and Yoshida (1969), and show no trace of any contaminating particles within the body of the flakes themselves. Further images of this type were obtained from thin sections cut perpendicular to the basal cleavage using the method of Brown and Jackson (1973). One of these is shown in Figure 2(d). However, the interpretation of these images was open to some question as their spacing invariably corresponded to the 10Å spacing of mica, suggesting in fact that these images were due to the illite impurity. Spot analyses in the analytical electron microscope seemed to confirm this, and a full discussion of images of this type will be made in a later report.

Mössbauer spectroscopy

The room temperature Mössbauer parameters of all samples are listed in Table 2. The spectra of DRP1 and LBH23 consisted of doublets having parameters compatible with the predominant presence of high-spin ferric ion in a six co-ordinated site (Bancroft, 1973), a typical spectrum being shown in Figure 3a. No significant changes occurred in the spectra at 80°K or following acid extraction. The spectrum of BSC1 was similar, except for the presence of ferrous ion (approximately 10 per cent) indicated by a small absorption at high velocities. Attempts to fit either single quadrupole doublets or two distinct doublets were not wholly satisfactory, and therefore it is probable that at least two sorts of ferric ion with very similar Mössbauer parameters were present, values quoted being averaged.

Spectra of samples GP2 and TPC1 at 290°K (Figure 3b) were characterised by a wide doublet corresponding to the ferrous ion together with an absorption at the center indicating ferric iron. In the 290°K spectrum of GP2 a shoulder was just resolved on the ferrous resonance at high energies and the spectrum was computer-fitted to two ferrous and one ferric quadrupole doublets. Following acid extraction both samples showed a marked diminution of the ferric signal relative to the ferrous signal, the

$$\frac{Fe^{3+}}{(Fe^{3+} + Fe^{2+})}$$

Table 2. Room temperature isomer shifts and quadrupole splittings (± 0·04 mm s^{-1}) for the samples studied. In most cases the parameters represent the average of a number of sites. Where only traces of the ferrous ion are present the corresponding parameters are not reported because reliable location is difficult. The samples GP1, TB146 and TB169 (very weak spectra) are omitted

Clay		δ mm s^{-1} (rel. −Fe)	Δ mm s^{-1}	$\frac{Fe^{3+}}{(Fe^{2+} + Fe^{3+})}$
BSC1	Fe^{3+}	0·36	0·52	>0·9
DRP1	Fe^{3+}	0·35	0·55	1
LBH23	Fe^{3+}	0·37	0·52	1
GP2	Fe^{3+}	0·35	0·67	0·56
	Fe^{2+}	1·12	2·88	
	Fe^{3+}	0·31	0·69	
TPC1	Fe^{2+}	1·01	2·71	
		1·14	3·14	
CCBH7	Fe^{3+}	0·37	0·61	1
LBH22	Fe^{3+}	0·36	0·56	>0·9
TB153	Fe^{3+}	0·39	0·48	1

ratio decreasing from 0·56 to 0·46 and 0·54 to 0·38 for GP2 and TPC1 respectively (Figure 3c). Isomer shifts and quadrupole splittings were compatible with the presence of the ferrous ion in a six co-ordinated site.

The remaining materials (CCBH7, LBH22, TB153 and TB169) all showed more complex behaviour indicative of magnetically ordered regions within the samples at 80°K. The room temperature spectra of

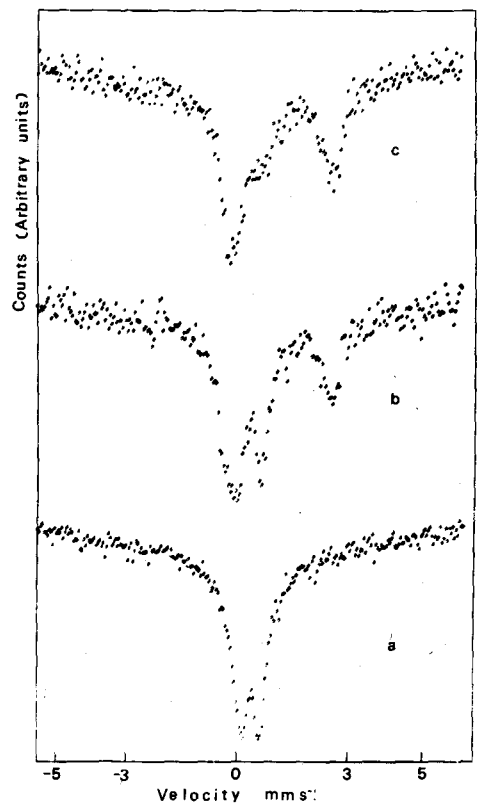

Fig. 3. (a) Room temperature Mössbauer spectrum of untreated DRP1. (b) Room temperature spectrum of untreated GP2. (c) Room temperature spectrum of acid-treated GP2.

https://doi.org/10.1346/CCMN.1975.0230505 Published online by Cambridge University Press

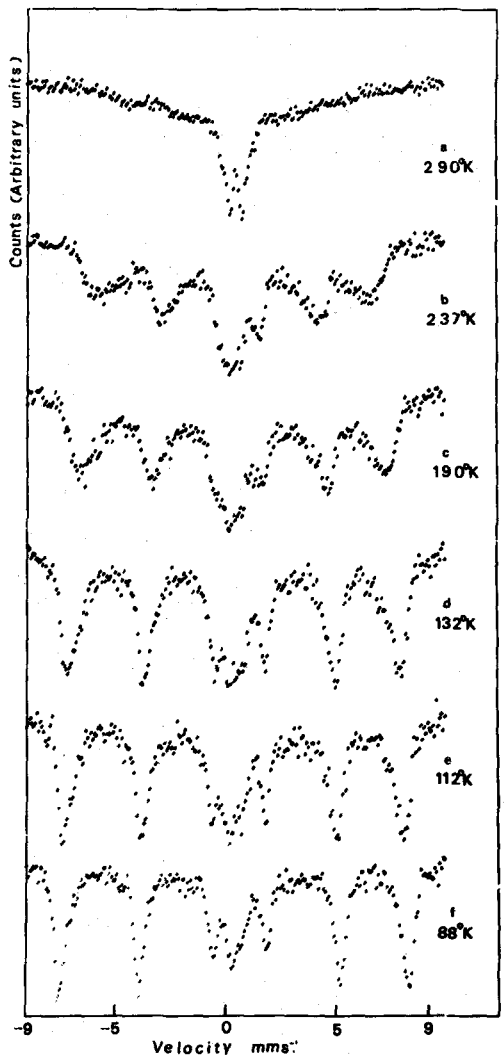

Fig. 4. Spectra of untreated CCBH7 as a function of temperature. Note the gradual appearance of a six-line pattern. Temperatures are accurate to ± 1°K.

LBH22 and TB153 consisted of a doublet attributable to the ferric ion with a small trace of the ferrous ion in sample LBH22. Again the computer fits to a single doublet were not completely satisfactory. The spectrum of LBH22 at 80°K contained a weak six-line pattern ($H_{int} = 490$KG) together with a residual central doublet. The corresponding spectrum of TB153 was very similar with a stronger six-line pattern and only a very weak residual central feature. Following acid extraction the six-line pattern at 80°K was no longer obtained in all cases.

The room-temperature spectrum of CCBH7 (Figure 4a) consisted of a central quadrupole doublet due to the ferric ion superimposed on a broad background. The latter altered at liquid nitrogen temperature to an intense six-line pattern ($H_{int} = 492$KG, $\epsilon = 0{\cdot}17$ mm s^{-1}) with a residual central singlet (in place of the doublet) with a pronounced shoulder at high energies. The sample was further studied in the temperature range 290°K to 80°K (Figures 4b to 4e). The resulting spectra showed how the broad background at room temperature gradually developed into a six-line pattern at the expense of the central doublet. This collapsing of the six-line pattern with increasing temperature is expected to arise when the relaxation frequency of the electronic spins (and hence the reversal frequency of the internal hyperfine magnetic field) is comparable with the Lamor precession frequency of the ^{57}Fe nucleus (Wickman, Klein and Shirley, 1966).

DISCUSSION

Classification of samples

Each of the methods of study effectively subdivided the samples into three main groups, with some overlap when comparing different methods. On the basis of chemical attack, the two South Carolina samples (BSC1 and DRP1) formed one group, being incompletely cleaned by acid. These samples were among the first group established by electron microscopy in that they possessed no form of observed surface contaminant. They also formed the first group established by Mössbauer evidence showing only a single ferric doublet at all temperatures. Because no form of surface contaminant was visible the iron present must therefore be situated in the kaolinite lattice substituting for aluminium in octahedral co-ordination. Since the samples were only partially cleaned it must be assumed that much of the iron is inaccessible to chemical attack and therefore distributed uniformly throughout the lattice.

Chemical attack studies placed the GP2 sample in a unique group due to its extremely rapid acid extraction. Electron microscopy confirmed this grouping from the apparently amorphous coating exhibited only by flakes of this sample. Mössbauer data, however, would tend to group this sample with TPC1. For this reason they are considered together. For these samples the picture is complicated by the presence of two types of the iron atom, the ferric ion evidently is more accessible to acid attack than the ferrous, as revealed in the Mössbauer spectra before and after acid extraction. If this is due only to the position of the iron atoms in the kaolinite lattice, it seems probable that the ferric ion is located closer to the flake surfaces than the ferrous. The much faster acid extraction of GP2, as compared to TPC1, could be explained by the fact that the ferric ion in TPC1 is in the crystal lattice predominantly near the surface, while a great proportion of the ferric ion in GP2 is actually present on the surface in the form of an amorphous coating. These two samples could therefore represent subsequent stages in a gradual process of oxidation and staining in which the ferrous ion is oxidised to the ferric and then migrates towards the flake surfaces (TPC1) and eventually forms an amorphous gel structure on the surface (GP2).

The final group as determined by chemical extraction tests consisted of all samples completely but slowly cleaned by acid treatment. Although TPC1 fell

https://doi.org/10.1346/CCMN.1975.0230505 Published online by Cambridge University Press

into this group it is best placed with the GP2 sample, as discussed above. The remainder of the samples TB153, TB169, LBH22, LBH23 and CCBH7) then form a reasonably consistent group. All can be completely cleaned. Therefore the iron present (virtually all ferric) must be accessible to chemical attack. For this reason LBH23 is included in this group regardless of its lack of surface contamination and a six-line Mössbauer spectrum at 80°K. In a manner analogous to that of the previous group the samples can be regarded as representing different stages in an overall staining process but the lack of any notable trace of the ferrous ion prevents any conclusions being drawn regarding the ferrous/ferric oxidation process. The LBH23 sample represents the first stage in the staining process, having the ferric ion in the lattice but near the flake surfaces, while in the LBH22 sample the first traces of a crystalline surface coating appeared as shown by the electron microscope evidence and the very weak six-line Mössbauer spectrum obtained at 80°K. The growth of a crystalline coating at the expense of the lattice located ferric ion then proceeded much further in the three remaining samples. The final stage was reached in the TB153 sample in which Mössbauer spectra indicated an almost complete absence of iron after acid extraction which suggests that virtually all iron present was incorporated in the surface coating.

Interpretation of Mössbauer spectra

From the relatively low total iron content of the clays studied the iron within the lattice can be expected to be magnetically dilute and only a paramagnetic doublet Mössbauer spectrum will be observed. The appearance of a six-line pattern in the low-temperature spectra of certain samples therefore implies regions within these samples where high concentrations of iron exist locally and because these patterns disappear following acid extraction such six-line spectra are associated with the surface contaminant. Lattice image studies prove that the contamination is crystalline and observed spacings are indicative of goethite even though at room temperature goethite is an antiferromagnet exhibiting a six-line Mössbauer pattern (Forsyth, Hedley and Johnson, 1968). No such pattern was observed at room temperature in any of the clays but in view of the small particle size (*ca.* 1000Å × 100 – 200Å) of the contamination the possibility that the particles are super-paramagnetic must be considered. The isomer shift of 0·36 mm s^{-1} and quadrupole splitting of 0·66 mm s^{-1} observed for the typically stained CCBH7 sample are in agreement with those of goethite above its Néel temperature (δ = 0·35 mm s^{-1}, Δ = 0·6 mm s^{-1}), but the internal magnetic field at the nucleus (H_{int} = 492KG) at 80°K is slightly smaller than that measured for bulk goethite (H_{int} = 500 ± 3KG, Van der Woude and Dekker, 1966). However, similar small reductions relative to the internal field for bulk samples have been observed for small particles of hematite (Gangas *et al.*, 1972). In addition, the quadrupole splitting deduced from the asymmetry of the six-line pattern at 80°K is compatible with the spins lying perpendicular to V_{zz} which is positive, as is the case for bulk goethite, and the partially collapsed spectra are very similar to those of goethite close to its Néel point. The Mössbauer evidence is therefore fully compatible with the presence of small super-paramagnetic particles of goethite which constitute the surface staining of this particular kaolinite, and the samples grouped with it.

Particle size determination

Under certain circumstances, it is possible to obtain particle size distribution from a Mössbauer study of super-paramagnetic particles as a function of temperature. For instance by measuring the temperature variation of the ratio of super-paramagnetic doublet to six-line pattern in the spectra of hematite it has been possible to measure the size and distribution of hematite particles in soils (Gangas *et al.*, 1972). In the case of hematite either a six-line pattern, a completely collapsed doublet or a superposition of both is observed. This is not the case with CCBH7 which exhibits only a partially collapsed spectra. This precludes a detailed examination of the particle size distribution but by comparing the spectra with calculated partially collapsed spectra as a function of spin relaxation time and by reference to previous work on super-paramagnetic particles of goethite by Shinjo (1966) some information can be obtained. The critical volume of a goethite particle which leads to a collapse at 290°K of the six-line pattern is 3×10^{-17} cm^3 (equivalent to spherical particles of 300Å diameter). The broad background of the CCBH7 spectrum at 290°K shows that the six-line pattern has not completely collapsed and therefore places a lower limit of 3×10^{-17} cm^3 on at least a fraction of the surface contaminant particles. By comparison of the wings of the spectra with calculated spectra it is possible to estimate (Kundig *et al.*, 1969) an upper limit of a kind of relaxation time for the spins of *ca.* 10^{-9} sec. From the relationship $\tau = (1/f_0)\exp(KV/kT)$, with $f_0 = 10^{10}$ c s^{-1} and $K = 10^4$ erg cm^{-3} (Shinjo, 1966), an upper limit of equivalent spherical particle diameter of *ca.* 10^5Å can then be deduced. This procedure applies to the particles contributing to the six-line pattern, but the residual central feature, although probably due to ferric ion within the kaolinite lattice, may arise from extremely small super-paramagnetic clusters of goethite still displaying a collapsed spectrum at 80°K.

CONCLUSIONS

1. Electron microscopy and Mössbauer spectroscopy have revealed three distinct types of staining in kaolinite minerals. All have some ferric ion substituted for aluminium uniformly throughout the lattice and in type a) all the iron is present in this form. In the other types the majority of the ferric ion is

https://doi.org/10.1346/CCMN.1975.0230505 Published online by Cambridge University Press

present as b) a crystalline coating of goethite or c) as an amorphous coating. The last type also contains ferrous ion substituting for aluminium within the lattice.

2. Acid extraction studies showed the impossibility of cleaning kaolinites with the first type of staining, although those in categories (b) and (c) could be cleaned with varying amounts of stain removal. Samples in category (c) with amorphous surface coatings proved to be cleaned very easily.

3. The percentage of iron removed by acid extraction gradually increases throughout the three categories above with virtually all iron being removed from samples with crystalline surface coatings. In kaolinites included in category (c) the ferric form was removed preferentially.

4. The finely crystalline particles of category (c) are probably super-paramagnetic and particle size estimates from the Mössbauer spectra based upon this assumption agree reasonably well with those observed in the electron microscope.

Acknowledgements—We wish to thank Professor J. M. Thomas and Professor W. Davies for their continued interest and assistance with this work and the Steetley Company Limited which provided many of the specimens. Thanks are also due to the Science Research Council for providing the Phillips EM-300 electron microscope and to JEOL (U.K.) Limited for use of their analytical electron microscope. One of us (D.A.J.) was in receipt of a Steetley Post-doctoral Fellowship which is gratefully acknowledged.

REFERENCES

Bancroft, G. M. (1973) *Mössbauer Spectroscopy*. McGraw-Hill, U.K.

Bates, T. F. (1971) The kaolin minerals. In *The Electron-Optical Investigation of Clays*. (Edited by J. A. Gard.) Chap. 4 pp. 109–157. The Mineralogical Society, London.

Brindley, G. W. (1961) Kaolin, serpentine and kindred minerals. In *X-ray Identification and Crystal Structures of Clay Minerals*. (Edited by G. Brown.) Chap. 2, pp. 51–131. The Mineralogical Society, London.

Brown, J. L. and Jackson, M. L. (1973) Chlorite examination by ultramicrotomy and high resolution electron microscopy: *Clays and Clay Minerals* **21,** 1–7.

Dowell, W. T. C. (1961) The observation of small crystal lattice spacings in the electron microscope: *J. Phys. Soc. Japan* **17,** *suppl.* B-II, 175–178.

Erickson, H. P. and Klug, A. (1971) Measurement and compensation of de-focusing and aberrations by Fourier processing of electron micrographs: *Phil. Trans. R. Soc. London* **B261,** 105–118.

Forsyth, J. B., Hedley, J. G. and Johnson, C. E. (1968) The magnetic structure and hyperfine field of goethite: *J. Phys. C Ser.* **2, 1,** 179–188.

Gangas, N. H., Simopulos, A., Kostikas, A., Yossoglou, N. J. and Filippalis, S. (1972) Mössbauer studies of small particles of iron oxides in soils: *Clays and Clay Minerals* **21,** 151–160.

Kundig, W., Kobelt, M., Appel, H., Constabaris, G. and Lundquist, R. H. (1969) Mössbauer studies of Co_3O_4 bulk material and ultra-fine particles: *J. Phys. Chem. Solids* **30,** 819–826.

Mackay, A. L. (1962) Akaganéite: *Mineral. Mag.* **33,** 270–280.

Mackenzie, R. C., Meldau, R. and Gard, J. A. (1962) Ageing of sesquioxide gels II: *Mineral. Mag.* **33,** 145–157.

Mackenzie, R. C., Follet, E. A. C. and Meldau, R. (1971) The oxides of iron, aluminium and manganese. In *The Electron-Optical Investigation of Clays* (Edited by J. A. Gard) Chap. 11 pp. 315–344. The Mineralogical Society, London.

Rooksby, N. P. (1961) Oxides and hydroxides of aluminium and iron. In *X-ray Identification and Crystal Structures of Clay Minerals*. (Edited by G. Brown.) Chap. 10, pp. 354–392. The Mineralogical Society. London.

Shinjo, T. (1966) Mössbauer effect in antiferromagnetic fine particles: *J. Phys. Soc. Japan* **21,** 917–922.

Suito, E., Arakawa, M. and Yoshida, T. (1969) Electron microscopic observation of the layer of organo-montmorillonite: *Proc.* 3rd *Int. Clay Conf. Tokyo* **1,** 757–763.

Van der Woude, F. and Dekker, A. J. (1966) Mössbauer effect in alpha-FeOOH: *Phys. Stat. Solid.* **13,** 181–193.

Wickman, H. H., Klein, M. P. and Shirley, D. A. (1966) Paramagnetic hyperfine structure and relaxation effects in Mössbauer spectra: ^{57}Fe in ferrochrome A: *Phys. Rev.* **152,** 345–357.